Design of the Next-Generation Autonomous Flying Ambulance

Ellande Tang*, Patrick Spieler†, Matthew Anderson ‡, and Soon-Jo Chung§
California Institute of Technology, Pasadena, CA, 91125

As electric aircraft take to the skies, it is becoming common to speculate on potential niches in which to apply the technology. One promising role for these vehicles is in the medical domain, a role currently filled by helicopters. A Vertical Take-Off and Landing (VTOL) aircraft with autonomous capabilities could avoid obstacles and transport injured patients to receive critical medical care more quickly than land-based options. This paper presents the design of a novel, fully-electric VTOL aircraft designed to satisfy a medical transport mission by carrying a patient and a paramedic a moderate distance. The paper also presents a scale vehicle model that can be used to test the vehicle design and potential autonomy technologies as well as the special design considerations unique to a VTOL with fixed-wing capabilities. The resultant vehicle will represent the state-of-the-art of what is possible with existing hardware while remaining a flexible platform for autonomy research.

I. Introduction

A desire for Vertical Take-Off and Landing (VTOL) aircraft has been present since nearly the dawn of aviation. While this role is somewhat filled by the helicopter, there is also a desire to have vehicles with this capability that can perform missions usually carried out by fixed-wing aircraft as well. The widespread increase in the presence of aircraft, particularly unmanned aircraft, in everyday life has meant that there is a strong need for the ability to field these aircraft without the large and costly infrastructure typically associated with fixed-wing vehicles. In particular, the electric VTOL (eVTOL) industry is one that is rapidly developing and growing. By 2030, it's estimated that the eVTOL market will be worth anywhere from the hundreds of millions USD [1] to the billions [2].

While fossil fuel-powered vehicles were the norm for many decades, the development of new electric batteries, robust electric motors, and advanced flight controllers have led to electric propulsion becoming the technology of choice in hobby aircraft and for it to become an increasingly appealing technology in general for commercial aviation. The potential for lower component and maintenance costs, accessibility of components for prototyping, and the benefits of distributed electric propulsion also incentivize the shift to electric [3].

A. Utility of Helicopters in Medical Settings

Helicopters have a long history of use in the medical setting, dating back to the Second World War where casualties were evacuated from combat zones. Even today, helicopters are used extensively for medical transport, with an estimated 400,000 missions being flown each year in the US alone [4]. Helicopters can transport injured people from areas of limited accessibility, such as hikers in rough terrain. Despite helicopters often being the best possible option in this context, they still face a number of serious drawbacks. They are often unable to land next to the patient due to a combination of the terrain and the rotor size. In fact, helicopters often simply dangle a stretcher [5], which is used to transport the patient to an ambulance on the ground. Helicopters and their pilots also represent a significant financial burden [6], costing $1M per year per vehicle to maintain, making their value in urban settings with alternative infrastructure questionable.

During the 1980s, it is estimated that there were as many as 12,000 Emergency Medical Services (EMS) vehicle crashes in the US every year, and transportation-related fatalities among EMS workers is significantly higher than any other emergency service workers [7]. In addition to the recorded crashes, each crash in this period tended to cause approximately four "wake effect" collisions involving other vehicles. Shifting medical services to the air could help reduce the injuries associated with EMS efforts.

Medical transport has an established tendency to skew the risk assessment abilities of pilots, leading to incorrectly weighing the dangers of more typical flight hazards. In fact, it is common to simply not inform the pilot of the patient's

medical condition [8], as risking the lives of the pilot and crew in addition to the patient is not a safe practice. Removing the pilot from the equation and reducing the on-board crew would help mitigate the risk associated with air medical services and minimize loss of life in the event of an accident.

B. The Autonomous Flying Ambulance

This paper presents the fourth generation of Caltech's Autonomous Flying Ambulance (AFA), shown in Fig. 1 in the flying configuration, and Fig. 2 in the hovering and storage configuration with the wings folded upwards. The AFA was designed from the ground up to support medical missions in both urban and remote environments.
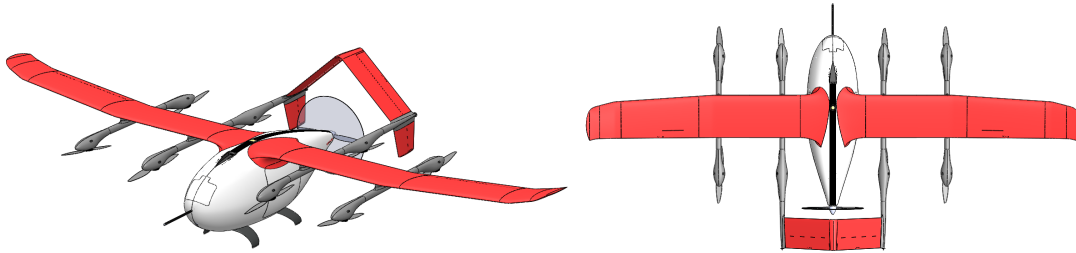

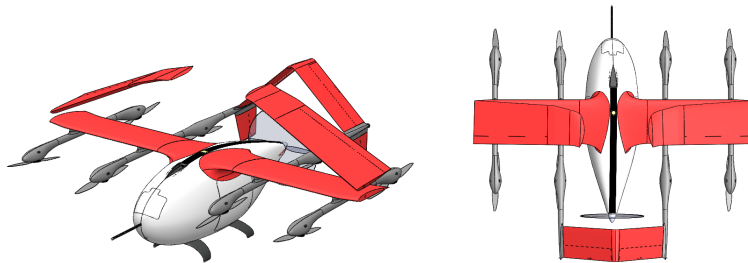Fig. 1   Inclined and top views of Caltech's Autonomous Flying Ambulance (Version 4).

Fig. 2   Inclined and top views of Caltech's Autonomous Flying Ambulance with the outer wing sections folded for reduced landing footprint and storage.

This paper will describe the features of the next generation of the Autonomous Flying Ambulance, including the full-scale mission objectives (Section II), the preliminary design considerations, sizing and scaling methods (Section III), and the detailed design of the scale model (Section IV through Section VI). In Section IV the aerodynamic design aspects are presented, Section V discusses propulsion and power system design and in Section VI an overview of the autonomy and sensor components is given. The modelling methods for the unique challenges of VTOL flight will be explored in Section IV.C, and the design of failure-tolerant propulsion systems will also be addressed in Section V.A and V.B.

C. Prior Work

1. Existing eVTOL Designs

While every electric multi-rotor is an eVTOL, we will specifically examine those designs that use a wing to generate a significant portion of the vehicle's lift during flight. A number of commercial ventures are seeking to bring eVTOLs to market for passenger transport. Significant designs include those by Lilium [9], Airbus [10], Aurora [11], Hyundai [12], Uber [13], and Kitty Hawk [14]. In the air ambulance domain, AMSL Aero have recently unveiled their Vertiia which is planned to have both battery and hydrogen variants to support medical missions [15]. These designs have a number of similarities, but also feature different aerodynamic arrangements and touted performance. Studies [16] to evaluate the theoretical performance of these designs has found the utility of each design depends heavily on the chosen mission profile.

The vehicle described will be the fourth iteration of Caltech's Autonomous Flying Ambulance. The first version was a bare-bones multirotor with a wing and tail used for basic controls development. Versions 2 and 3 (Fig. 3, described further in [17]) improved on the design by adding an aerodynamic fuselage and articulated wings. These vehicles served to help refine the project goals and system level design of the vehicle.
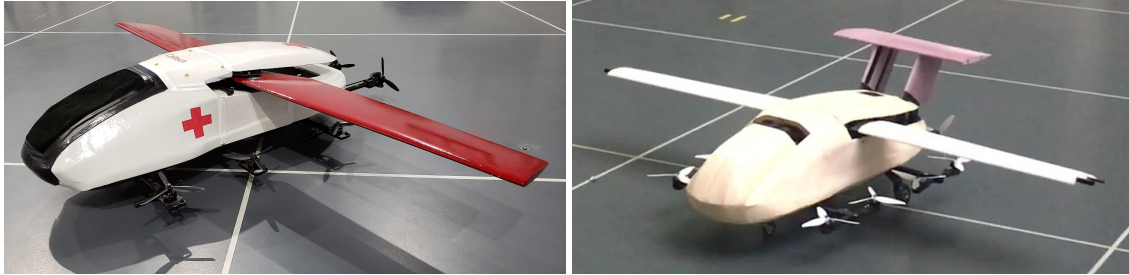

Fig. 3   Earlier designs (Versions 2 and 3) of Caltech's Autonomous Flying Ambulance.

Version 2 had a machined foam exterior, articulated wings for storage, and a pair of tilting rotors. Initial flight tests indicated that the rotors were undersized, the aerodynamic design was unstable, and that the tilting rotors introduced unnecessary complexity into the controls. While the vehicle was able to hover, it never achieved a complete transition to fixed-wing flight.

Version 3 sought to address many of these deficiencies. A wooden laser cut shell was used for the exterior to increase the internal volume and the tilting rotors were replaced by a set of fixed lifters and thrusters. The diameter of the rotors was increased to improve energy efficiency and a larger battery was installed. Guided by results from wind tunnel testing, a tail was added, as well as control surfaces for fixed-wing flight.

With the lessons learned, the fourth version of the AFA was designed from scratch as shown in Fig. 2. Part of this re-design process included a more robust power and propulsion system, a composite structure, and a enhanced patient transport bay. With these improvements, we aim to produce a vehicle that represents the state-of-the-art in aerial ambulances, and build a sub-scale model that can perform as an effective technology demonstrator and research testbed.

II. Requirements of a Flying Ambulance

In order to create a vehicle useful for medical purposes, there are several criteria to meet. We propose that such a vehicle would need to hover for around 8 min to be able to takeoff and land safely (reserves inclusive). An effective range of 65 km (40 mi) was also proposed in order for the vehicle to have a useful coverage area. As shown in Fig. 4, this range in a major city such as Los Angeles would allow it to comfortably reach much of the urban area from a centrally-located hospital. The proposed payload is two passenger – one patient, and one medic who can easily access the patient en route to provide medical care. For sizing, we designed the craft around two 95th percentile males in both dimension and weight [18].

Most eVTOL vehicles are designed for either passenger or cargo transport, operating regular, pre-approved routes. Operating out of 'vertiport' hubs, the take-off / landing area is fully prepared ahead of time. This requires a massive investment in infrastructure, with Lilium projecting costs for their vertiport hubs between $1M for basic landing zones and $18M USD for a major rooftop hub [19].

A flying ambulance, however, cannot be expected to operate from a pre-prepared area, and instead must be able to land in any reasonably open space, minimising the distance to the patient. The ambitious goal of being able to fit within two standard US highway lanes was chosen. This enables the AFA to land on roads and highways (Fig. 5), and operate most places a standard road-based ambulance could, but without the need to contend with traffic. On returning to the hospital, existing roof-top helipads could be used, or, due to the small landing profile, a fenced off area in the parking lot.
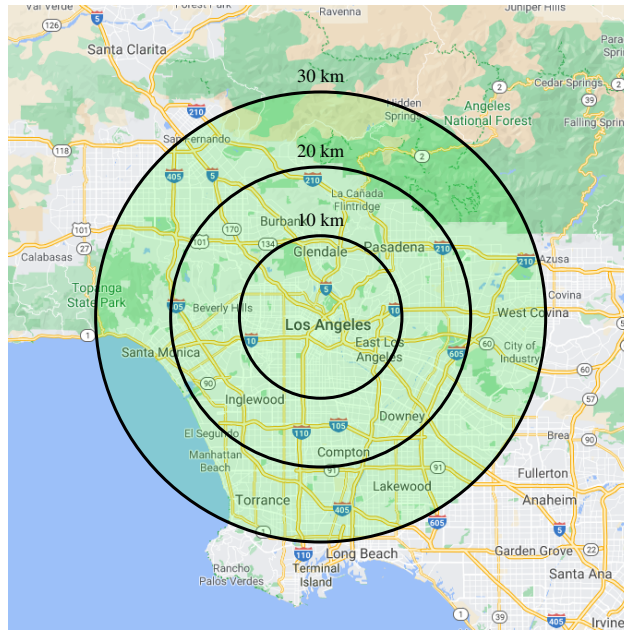
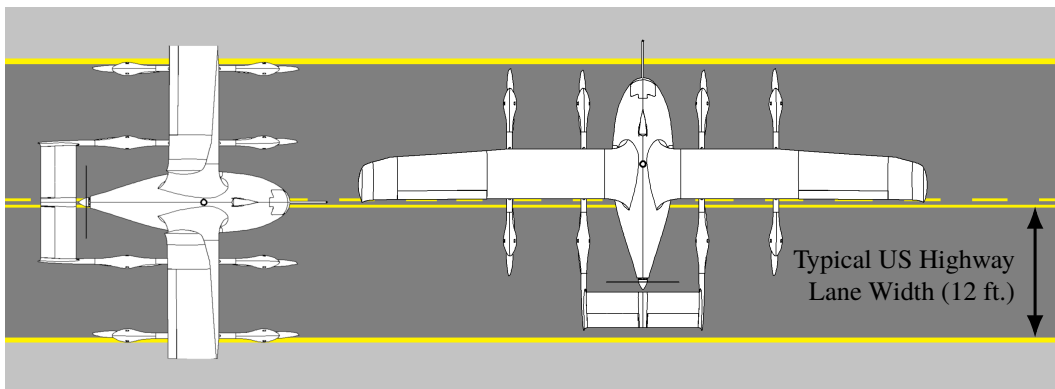**Fig. 4   Map of Los Angeles demonstrating coverage of a 30 km range.**

Fig. 5   AFA pictured on standard US highway lanes (folded and un-folded wing configurations).

III. Preliminary Design

A. Configuration

The fourth generation of the AFA keeps the hybrid multirotor/aircraft quadplane configuration of the previously designed AFA generations. A quadplane (a fixed-wing aircraft with non-tilting lifting propellers to add VTOL capability) is ideal for the VTOL air ambulance mission as it provides safety through multiple propulsion systems, is mechanically simpler than tilt-rotor systems, and, unlike tail-sitter configurations, enables the passengers to remain level throughout the flight. The primary configuration change compared to previous versions was to move the powered-lift motors to the wings, enabling dual sliding access doors on the side of the fuselage and improving the ergonomics and accessibility of the payload/patient bay. This configuration also allows for the use of larger diameter propellers, opening up the design space.

The change to the wing-mounted powered-lift system also drove the design towards increasing the number of powered-lift motors. Six motors represent the typical lower limit of number of motors to provide redundancy to a motor failure, as any fewer (assuming a standard, fixed-motor configuration) leave the yaw moment unbalanced – a highly undesirable case for a passenger-carrying vehicle. Distributing six motors well on a quadplane however becomes difficult, and hence drove the design to a multiple of four motors, with a minimum of eight.

4

Table 1 Specs for the Full and 1/5ᵗʰ Scale AFA Vehicles. Values are taken at sea level and include 20 % battery reserves. Nominal values are for the design mission, maximum values are for the pure hover (80 % hover) and pure fixed-wing (60 % cruise, 20 % hover) cases.

		Full Scale		1/5ᵗʰ Scale	
		Nom.	Max.	Nom.	Max.
Wingspan	[m]	15		3	
Wingspan (Folded)	[m]	7		1.6	
Mass	[kg]	1350		16	
Cruise Speed	[m/s]	45		24	
Range	[km]	65	109	15	27
Endurance (Hover)	[mins]	8.0	13.8	3.7	6.4
Endurance (Fixed-Wing)	[mins]	24	40	14	19

B. Preliminary Sizing

Aircraft design is a high-dimensional, complex multi-disciplinary design problem. A fine balance needs to be struck between a host of parameters such as the weight of the components, the area and span of the wings, the size and number of propellers, the length of the tail, etc., where a change in one component can cascade through and require modifications to match throughout the rest of the aircraft. To narrow the design space and enable the detailed design of each component of the AFA, an in-house optimization code was used to provide an approximate size, configuration, and weight distribution for the aircraft.

The optimization variables included the wing and tail geometry, motor and propeller sizes, battery capacity, structural weights, and aerodynamic flight conditions in cruise. The models of the battery and the motors were based on a model derived from COTS components. To estimate the weight of the carbon fiber composite structure, the optimizer includes critical structural loads in fixed-wing and hover flight. Drag estimates of significant components are used to size the forward-flight motor and estimate the energy consumption in fixed-wing flight. The hover power consumption and the motor sizing were based on the ideal aerodynamic induced power from disc actuator theory and a propeller Figure of Merit (FoM).

Using these models, a hybrid VTOL can be sized for various mission requirements and optimization objectives. For the AFA, the optimization objective was the landing footprint of the vehicle, given a fixed payload, mission endurance, and range constraints. A small landing footprint has always been a critical design goal of the AFA series (Section I.C.2) to maximize their possible landing locations in urban environments. To reduce the footprint, the outer wings fold up before landing (Fig. 2), making the rotor diameter the main driver of the vehicle size. For this reason, the optimization objective was to minimize the lifter rotor diameter, subject to the mission constraints.

The resulting design of AFA has a 15 m wingspan, 1.5 m diameters lifter rotors, and an estimated weight of 1 350 kg (including 220 kg of payload). The AFA was designed to have an optimal cruise speed of 160 km/h, and is capable of carrying two passengers for 65 km with an additional 8 minutes of hover endurance.

C. Scaling for a 1/5ᵗʰ Prototype

Prior to construction of a full-sized AFA, a scale technology demonstrator was developed. Several different scales were considered, but 1/5ᵗʰ scale (3 m wingspan) provided a good balance between volume for research hardware and overall size. A scaling of constant Froude number $Fr = V/\sqrt{lg}$, where V is a characteristic speed, l is a characteristic length, and g is the acceleration due to gravity, was chosen for our scale vehicle since such a scale model captures the inertial and gravitational effects of the full scale (assuming compressibility effects are negligible) [20]. In particular, a Froude number scaling will result in a scaled turn-radius for the same load factor and bank angle.

According to this scaling method, a 1/5ᵗʰ scale vehicle would have a target weight of 11 kg, a wingspan of 3 m, and a cruise speed of 20 m/s. However, since the scale model will also be used for autonomy and controls research, the target weight was increased to accommodate a larger payload mass. The maximum takeoff weight was increased to 16 kg, and includes 3 kg of payload. A mass-breakdown of vehicle weight showing the major subsystems is shown in Fig. 6.

Based on the vehicle weight and the choice of propulsion system and battery, the 1/5ᵗʰ scale vehicle has a predicted
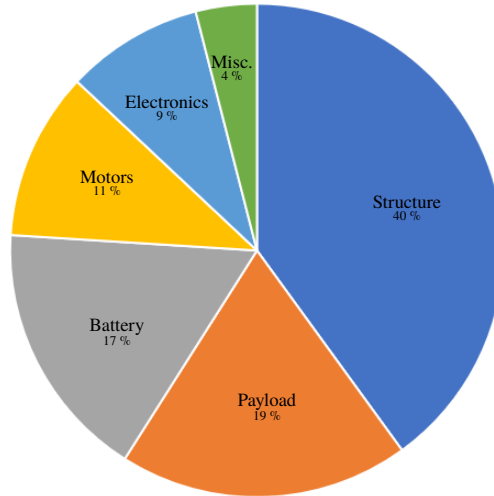
Fig. 6   Mass breakdown of the 1/5th scale vehicle.

range of 22 km using half the battery capacity for cruise. In hover, the vehicle has an endurance of about 6 minutes with full payload (with 20 % battery capacity as reserve).

D. Design for Use as a Research Platform

The scale AFA is designed to be both a technology demonstrator and a research platform for testing next-generation autonomous flight guidance and controllers, such as machine learning-based methods [21–24]. As such, the most likely failure modes for the AFA are expected to be in software (both in low-level control and higher-level autonomy) and hence the AFA needs to be designed to be robust against these failures [25]. Failures in autonomy typically happen shortly after initialization/entry into a particular flight mode (such as switching from fixed-wing to hover), meaning pilot reaction times can be expected to be quick as the critical period is short-lived and at a known time. Unfortunately, these critical periods often occur during risky flight regimes (low speed, low altitude), meaning there is little energy or time available to execute the recovery.

By design, the quadplane configuration of the AFA allows for an effective virtual parachute (commonly known as a quadchute) to be implemented where the vehicle can be 'caught' and recovered at any time on the lifter motors. The lifter layout is designed such that even in the event of a lifter motor failure, the vehicle remains fully controllable (explained in detail in Section V.B). In cases where the failure causes the virtual parachute to be ineffective (such as a loss of lifter power), the AFA is aerodynamically designed to be as recoverable as possible through manually-piloted control. Features such as a benign stall, departure resistance and good spin recovery characteristics (explained in more detail in Section IV.B) all contribute to helping the AFA naturally recover from adverse flight conditions.

Future work will include automating the fall-back from research-to-COTS control logic and will be implemented on a separate flight controller to give a completely redundant fall-back control architecture. This means the switch back to 'reliable' control can happen more quickly than the pilot can react, and dangerous conditions that may not be immediately obvious to ground observers (such as state estimators becoming unstable or on-board sensors suddenly failing) can be detected.

IV. Aerodynamic Design and Stability Analysis

A. Fuselage Design

As the primary volume for component storage within the AFA, special attention was given to the interior and exterior design of the fuselage. While roughly tear-drop shaped, we were unable to make the body symmetric about its axis due to propeller clearance and wing-fuselage interfacing. The interior space allows for two 95th percentile males (roughly 1.87 m in stature) to fit, one sitting (the paramedic) and one lying down (the patient), as shown in Fig. 7. Efforts were made to ensure that there was sufficient space for the passengers, accounting for the structural elements of the wing,

wall thickness of the fuselage, and proximity to the access doors on the side of the aircraft.
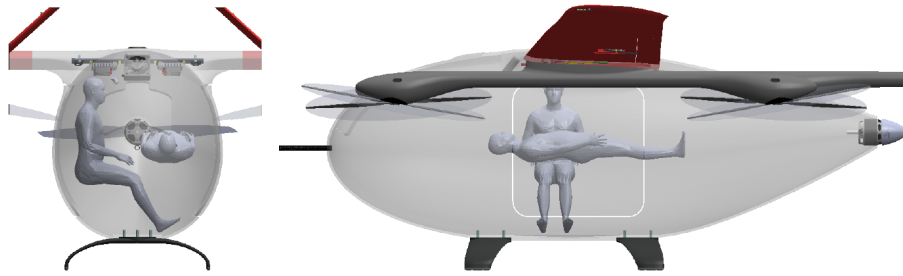

Fig. 7   95th percentile passengers (patient and paramedic) as they would fit within the fuselage.

Where possible, the design of the AFA was optimized to minimize drag. Due to the relative size of the payload compared to the chosen vehicle dimensions, the fineness ratio of the fuselage is quite low. Due to the low fineness ratio, flow separation from the fuselage is likely to happen. This flow separation is mitigated by the upstream effects of the aft propeller, and the trailing surfaces are designed to not exceed more than 30 degrees from the nominal flight direction [26].

CFD analysis was also carried out on the 1/5th scale fuselage design to evaluate the design's drag characteristics. Figure 8 shows the results of the analysis on the fuselage, visualizing the shear stress vectors on the surface. The results indicate that the fuselage appears to have relatively long runs of laminar flow over the surface at the nominal flight conditions. The strong tapering towards the aft causes a region of flow separation, but there is subsequent reattachment as the flow transitions to turbulent. The addition of the inflow of the pusher propeller helps mitigate more aggressive flow separation by energising the flow, as shown in Fig. 9.
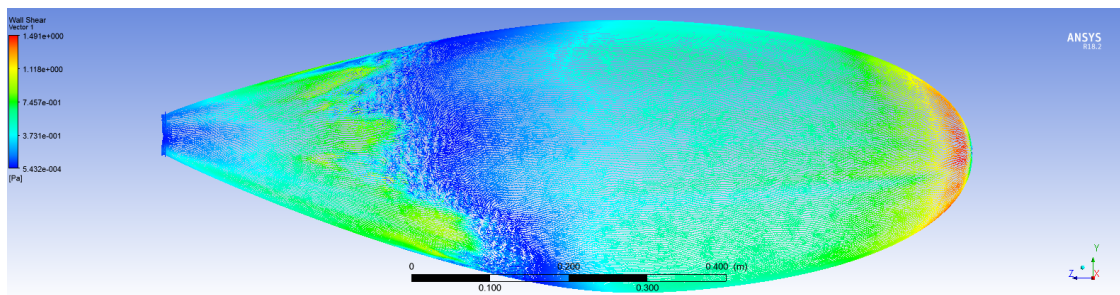

Fig. 8   CFD of the fuselage design with shear stress vectors shown.
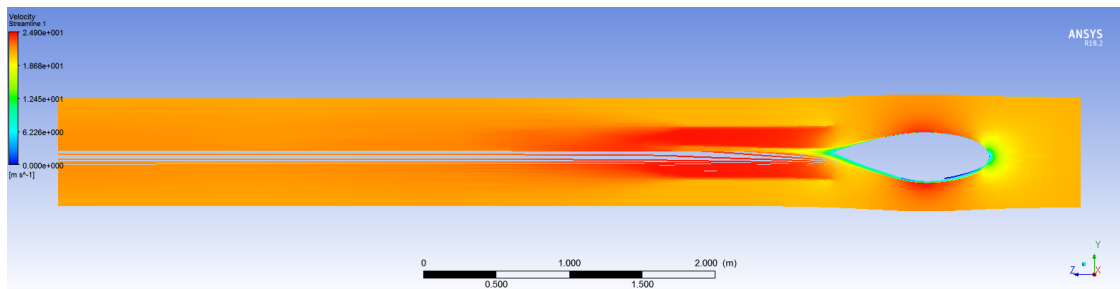

Fig. 9   CFD of the fuselage design with center plane streamlines shown. The effect of the aft propeller is visible.

Quadplanes do not require a traditional landing gear with wheels (only streamlined 'legs' are required) as take-off and landing is completed without a ground roll, and this eliminates a significant source of drag and weight. Fixed, as opposed to retractable, landing gear was also selected as the drag reduction was judged not to offset the weight penalty

of the required retraction mechanism. As a research vehicle, ideal landings are not guaranteed and hence the landing gear is attached using bolts that will shear out in the event of a belly landing. This means the landing gear is able to shear away from the fuselage without damaging the internal structure and the fuselage can be used to distribute the landing loads over a larger area.

B. Traditional Stability and Control

The design of a VTOL aircraft offers much more freedom than for a traditional aircraft in that a typical major design driver, take-off and landing performance, can mostly be ignored. In particular, this allows for the aerodynamic surfaces to be sized to have a higher stall speed (speed at $C_{L_{stall}}$), reducing the size and overall weight of the surfaces. This was captured as part of the optimizer routine which specified the wing area, aspect ratio and cruise lift co-efficient, leaving the wing shape, airfoils, control surfaces and tail design to be determined.

The AFA was modelled (as shown in Fig. 10) using OpenVSP [27], an open-source design and aerodynamic analysis tool developed by NASA. In addition to a vortex-lattice method (VLM) aerodynamic solver, OpenVSP features a panel method solver, enabling the effect of the large fuselage to be captured during the stability analysis. Validation calculations between the two solvers were performed using identical geometries to determine if the less-computationally-expensive VLM method would sufficiently capture the effects of the fuselage. For the quantities of primary concern (the static stability derivative C_{m_α} and the weathercock stability derivative C_{n_β}), the VLM and panel methods both predicted very similar quantities over the expected operating C_L of the aircraft. As such, design work was conducted with the VLM solver and was periodically re-compared against the panel solver results.
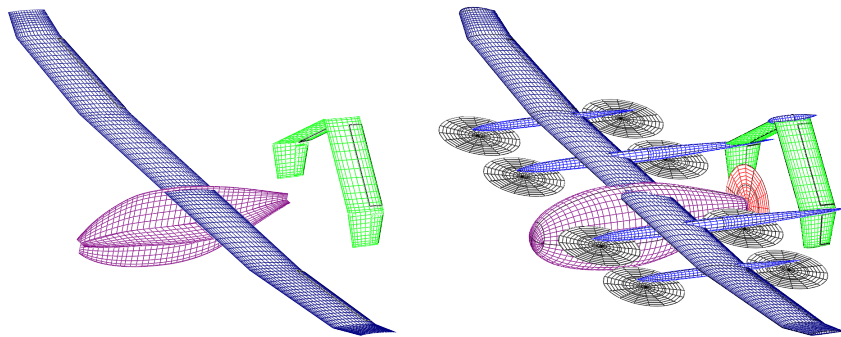

Fig. 10   VLM and panel models for the scale AFA model.

As the aspect ratio and wing area were determined from the scaling of the full-size model, the detailed design focused on the planform and twist of the wing. The three-part Schumann wing planform was chosen as it is easy to manufacture, has a reasonable span efficiency, and gives the aircraft a sleeker look than a standard rectangular wing. The increasing taper and reduced chord towards the wingtips however gives the planform poor stall characteristics, which, without washout, means there is a tendency for the wing to tip stall. The twist of the wing was designed to more evenly spread the lift across the wing during cruise, and benign stall characteristics were introduced with 3 deg of washout at the tips. While designing a wing with increasingly-cambered airfoils towards the wingtips widens the 'efficient' operating envelope [28], a single airfoil type across the span was chosen to simplify analysis, which improves utility for research work. The wing airfoil was chosen by matching the drag bucket of the airfoil to the cruise C_L and Reynolds number (using data from [29]), with a minimum allowable thickness ratio to provide bending stiffness and space to route cabling. The point in the wing where the taper begins acts as a break to disassemble the wing for transport, and is where the wing folding mechanism will be installed. Dividing up the wing here also introduces the possibility for alternate versions of the outboard wing to be installed if desired. This allows for the AFA to evolve into the future to support changing research needs.

Multiple configurations were explored for the empennage configuration (see Fig. 11). Each empennage configuration was sized to give approximately the same stability values (primarily by matching C_{n_β} and the horizontal tail volume coefficient), with the trailing edge of the fins placed at the most rear-ward position available. The large side-projected area of the fuselage fore of the CG, coupled with the short lever arm of the vertical tail, dictated a significant vertical tail volume coefficient, typically in the order of 0.10 to 0.12 (by comparison, General Aviation (GA) aircraft are typically around 0.02-0.04 [26, 30]).
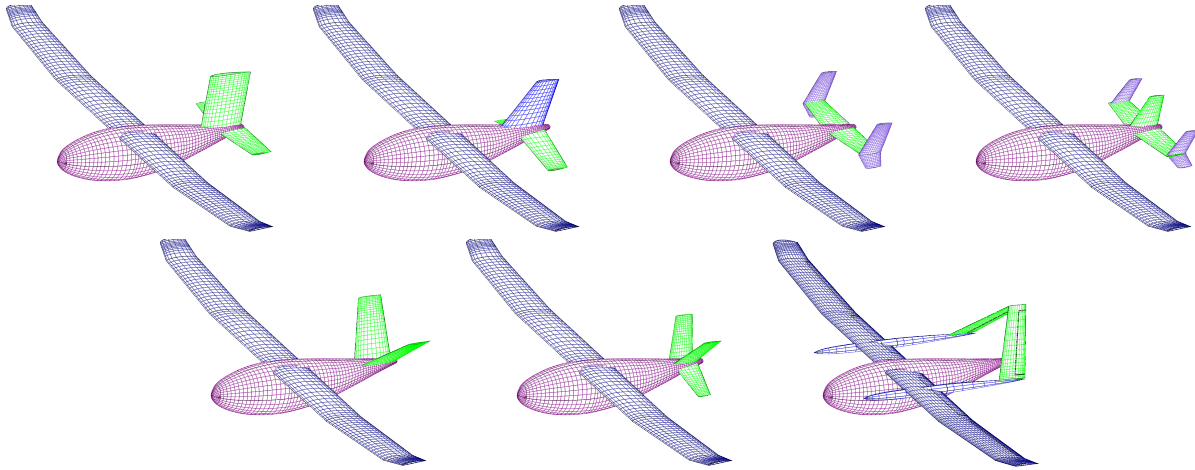
Fig. 11   Alternate empennage configurations explored.

Departure susceptibility (the tendency for the aircraft to enter a spin) and the ability to recover from a spin were a key design driver for the tail configuration as much of the intended research for the AFA is around the transition phase of flight. The departure susceptibility was estimated using the Lateral Control Departure Parameter and the dynamic yaw stability parameters [26]. Secondary considerations for the empennage configuration included keeping the vertical height to a minimum, ground clearance in case of a tilted landing, weight and overall aesthetics. A comparison of the base drag of each configuration (based upon the wetted area) showed each configuration added between 28 (A-tail) and 41 (Constellation-style Tri-Tail) drag counts on top of the approximately 300 drag counts for the rest of the vehicle, hence the drag was considered 'similar enough' between each configuration.

The A-tail configuration was chosen as it efficiently achieves the required weathercock stability at a minimum weight by re-using the already-invested structure of the lifter rails to mount the fins. Additionally, the A-tail enables the fuselage to be shortened while keeping the original tail lever arm, enabling the thruster motor to be brought closer to the CG and hence increasing the flexibility with weight and balance. The A-tail also has very good departure resistance, and spin recovery is possible as the tail control surfaces remain out of the wake produced by a spin. Further modifications to the A-tail configuration were made and additional vertical fins below the lifter rails were added, reducing the overall height of the vehicle and helping to de-couple the roll/yaw dynamics.

The control surfaces were sized as per the standard techniques [26, 30]. To support the research tasks the scale AFA model will carry out, more aerodynamic control authority was built in than is typical, giving ample control around transition flight speeds. Non-primary control surfaces (such as flaps and spoilers) were not included in the design to reduce complexity and manufacturing costs.

C. Stability in Reversed Airflows

VTOL aircraft are expected to operate at all side-slip angles, not just around the typically zero degree case as for regular aircraft. As with traditional multirotors, high side-slip cases (up to ±180 deg) occur routinely when operating in powered-lift mode, especially when translating or hovering in wind. Multirotors deal with these cases with ease – their reasonably axis-symmetric shape and lack of lifting surfaces mean there is little aerodynamic moment generated to return the vehicle to a 'nominal' orientation. VTOL aircraft like the AFA however have large lifting surfaces designed to support the aircraft in fixed-wing flight and to provide restoring moments in response to gusts and other disturbances. These lifting surfaces effectively work to destabilise the aircraft away from any operating condition that is not the zero side-slip case, severely limiting the flight envelope in which the aircraft can fly.

Determining the magnitude of the aerodynamic forces generated in backwards flight is important for predicting safe flight envelopes for the AFA. Simply setting the side-slip angle to 180 deg violates the small angle approximations used by both VLM and panel methods. Hence, the AFA was re-modelled 'backwards' in OpenVSP as shown in Fig. 12. These simulations showed the AFA to be significantly more unstable at 180 deg of side-slip than simply taking the negative of the 0 deg side-slip case. Several different configurations and designs were trailed to try and reduce the destabilising moments while flying backwards, however they all (as expected) unacceptably reduced the stability in
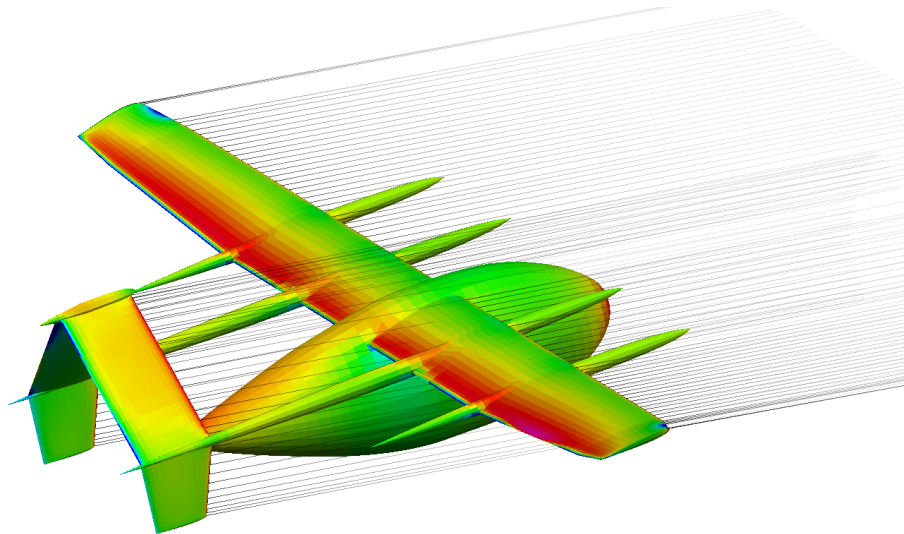
Fig. 12   AFA modelled for backwards flight.

forward flight. Another potential solution was to use deployable fins that could actively change the stability in flight (such as in [31]) but the additional complexity was highly undesirable.

To counter the destabilizing yaw moments while flying backwards, the AFA was designed to have significantly more yaw authority available from the lifter motors than a traditional quadplane. As outlined in Section V.A, the canted rotors enable a component of the strong thrust force to boost the relatively weak propeller drag torque-generated yawing moment. This provides the AFA with a much larger ability to resist the destabilizing aerodynamic yawing forces, enabling flight in higher-speed reversed airflows. Furthermore, emphasis on weather-cocking the aircraft into the wind while translating under powered-lift mode and hovering significantly reduces the need to design for reverse-flow conditions, and only marginal reduces the effective capabilities of the AFA.

V. Propulsion and Power

The AFA features independent propulsion systems for the powered-lift and fixed-wing modes of flight. Powered-lift is achieved through eight lifter rotors powered by direct-drive brushless electric motors that are independently controllable. For fixed-wing flight, the lifter motors are not required and a single pusher propeller driven by a direct-drive electric brushless motor is used. While the simplest design involves arranging the propellers symmetrically with parallel thrust axes, careful choice of inclinations can improve the vehicle's controllability and robustness to rotor failure with minimal effects on overall efficiency [25]. The design and hardware selection of the propulsion and power system for the scale model are outlined in the following sections.

A. Lifter Controllability

By appropriately tilting the 8 lifter rotors, full 6-DoF control can be achieved by the AFA. In particular, the AFA is able to generate side forces without needing to change its attitude, an important feature for a vehicle with high inertias like a quadplane. The ability to maneuver while staying level reduces the risk of a wing or tail strike, and increases the control bandwidth available to the aircraft to better handle gusty winds while hovering. In addition, tilting the lifters allows for improved yaw authority. Requirements for yaw authority are determined by the expected aerodynamic moments described in Section IV.C.

For a symmetric configuration, there are 4 independent variables to determine the tilt angles of the lifter propellers – the tilt magnitude and direction for both the inner and outer sets of propellers. We optimize the rotor orientation by seeking the lowest maximum motor thrust across all lifter motors (u_j, $j = 1, \ldots, 8$) for a set of maneuvers, such that:

$$\min_{\text{tilt config.}} \quad 0.7 \max_{j=1,\ldots,8} u_j^{\text{hover}} + 0.1 \max_{j=1,\ldots,8} u_j^{\text{hover \& roll-torque}} + 0.1 \max_{j=1,\ldots,8} u_j^{\text{hover \& pitch-torque}} + 0.1 \max_{j=1,\ldots,8} u_j^{\text{hover \& yaw-torque}}$$

subject to constraints:

- no mechanical interference between the rotor disks and the booms
- side force in hover $\geq$ 0.1 g acceleration
- side force in hover while applying a moment rotating the craft in the same direction $\geq$ 0.1 g acceleration
- yaw moment while applying roll & pitch moments in hover $\geq$ aerodynamic moment in reverse flight
  at airspeed = 10 m/s & sideslip = 10 deg (based on analysis in Section IV.C)

$$(1)$$

Each maneuver has a different relative importance, weighted using coefficients on each manoeuvre. The goal of the cost function is to produce a balanced control allocation where no single motor is overloaded. Additional optimization constraints are imposed based on desired system performance and mechanical constraints. The resulting configuration is shown in Fig. 13. The arrows indicate the horizontal component of the tilted thrust vectors. The tilt angle is 11.3 deg for all 8 rotors, which corresponds to only a 2 % required thrust increase in hover.
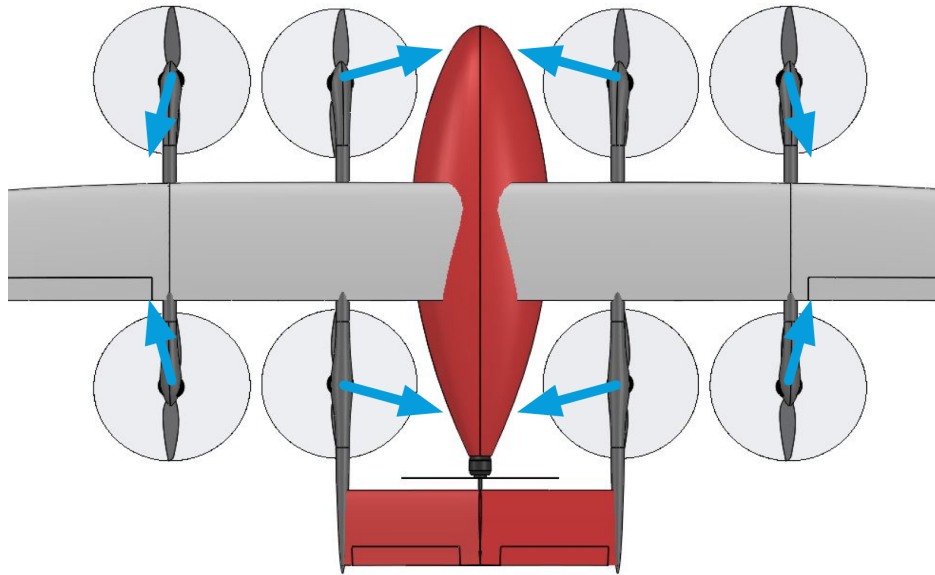

Fig. 13   Top view of the optimized thrust tilt directions.

B. Lifter Fault Tolerance

To be tolerant to an unknown motor failure, the AFA has to be trimmable to hover thrust with zero torque without saturating any of the thrusters and without changing the thrust allocation mapping. This should give the angular rate controller with integral gain a chance to stabilize the vehicle after a rotor failure. With the optimized thruster configuration, the highest motor thrust to achieve trim after a single motor failure is 35 N. Our lifter system is designed to be capable of 41 N thrust per motor, leaving enough margin for control after an undetected motor failure.

C. Lifter Power System

A number of criteria were developed for the lifter propulsion system. For maneuverability, a 2:1 thrust-to-weight ratio at MTOW is imposed. The AFA should also be able to operate for more than 1 minute in the single-motor failure condition without overheating, and all previous design criteria should be met up to 1 000 m above sea level and at 30 °C ambient temperature.

The T-Motor 14x4.8 Carbon Fibre propeller selected for the AFA is rated for a maximum thrust of up to 49 N. This propeller will be driven by a MN501S-300KV brushless motor from the T-Motor Navigator series, which is calculated

to be able to operate at the AFA's maximum anticipated thrust (41 N) without overheating. To drive the motor, an APD120F3[x] 120A ESC from Advanced Power Drives is used.

D. Lifter Propeller Drag

During forward flight, the lifter propellers do not actively contribute to the performance of the aircraft, cannot be feathered (in the traditional sense), and potentially produce a significant amount of drag if they stop in an unfavourable orientation. Furthermore, the drag created by the lifter propellers while in cruise is proportional to their size [32], creating yet another trade-off between high powered-lift efficiency and low cruise drag. One solution proposed by [33] is to retract the propellers into the motor pods for the cruise phase of flight. The gain in endurance using this method is highly dependent on the cruise airspeed – while [33] projected a potential 10 % increase in flight time for a manned aircraft, the significantly lower airspeeds of an unmanned vehicle mean the endurance is only improved somewhere between 1-6 %. Hence, the added complexity (and associated failure modes) of adding such a system was not justifiable for an initial scale prototype.

Another potential solution for minimizing the drag of the lifter propellers to to automatically align them to a favourable direction during cruise. This capability has already been demonstrated in vehicles such as that presented in [34], however sparse information is available of how to achieve this capability. With the increasing popularity of the quadplane configuration, it is anticipated that this functionality will be available in COTS ESCs in the near future, and the ESCs can easily be replaced as these features become available.

E. Thruster Power System

The thruster system was chosen based on several criteria such as indefinite operation in level flight at C_L of 0.4, and 20 s accelerated flight at 0.2 g from hover up until a cruise C_L of 0.6. The 15x8 Sport Series propeller from APC was selected and will be driven by a AT4120–250kV brushless motor from T-Motor. To drive the motor, a T-Motor FLAME 80A HV V2.0 ESC is used.

F. Energy Storage

To achieve the required RPM with the selected motors, a drive voltage of around 40 V is needed. The AFA's power consumption at MTOW and 1 000 m altitude in hover is 3 kW with a maximum peak of 10.5 kW (8.2 kW for the lifters and 2.3 kW for the thruster) at full throttle. The design battery is a 12 cell LiPo with a capacity of 9 Ah (400 Wh), a continuous discharge of 25 C (10 kW), and peak discharge of 50 C (20 kW). The installed battery pack is made up of two 9 Ah 6S Tattu batteries in series with a total battery weight of 2.5 kg.

VI. Sensors, Control, and Autonomy

As the AFA was developed as an autonomy testbed, it includes a variety of sensors. Some of the autonomous scenarios envisioned for the aircraft are inspection of volcanoes and mapping of remote islands. Therefore, the AFA includes additional payload space for other sensors as well. The payload volume is at the center of the vehicle and is easily accessible through the side doors.

The hardware architecture can be seen in Fig. 14. The vehicle includes two GNSS receivers for heading and position as well as space to mount downward looking cameras (for autonomous landing), a LIDAR range-finder and a front-facing RADAR (for collision avoidance). In addition, there are two flight computers (Pixhawks) to increase redundancy and to safely run experimental flight control algorithms as described in Section III.D. An on-board, Linux-based computer running ROS interfaces with the Intel stereo-vision camera used for Visual-Inertial Odometry (VIO).

The AFA is designed to run an adaptive nonlinear VTOL controller developed in our research group at Caltech [21]. This baseline controller requires a compact, custom-made 3D airflow sensor. The sensor is capable of measuring angle-of-attack, angle-of-sideslip, airspeed, static pressure. This sensor, together with the control algorithm, allows the vehicle to be fully controlled during the transition between hover and fixed-wing. Further, learning-based nonlinear flight control methods [22] along with a learning-based motion planner [23, 24] will be tested.

Acknowledgments

Fig. 14 Block diagram of the electrical system of the AFA scale model.

References

[1] Market and Markets, "eVTOL Aircraft Market," `https://www.marketsandmarkets.com/Market-Reports/evtol-aircraft-market-28054110.html`, 2019.

[2] BIS Research, "Global Electric VTOL (eVTOL) Aircraft Market to Reach $1.9 Billion by 2035," `https://www.prnewswire.com/news-releases/global-electric-vtol-evtol-aircraft-market-to-reach-1-9-billion-by-2035--300984170.html`, Jan. 2020.

[3] Kim, H. D., Perry, A. T., and Ansell, P. J., "A Review of Distributed Electric Propulsion Concepts for Air Vehicle Technology," *2018 AIAA/IEEE Electric Aircraft Technologies Symposium, EATS 2018*, Institute of Electrical and Electronics Engineers Inc., 2018. https://doi.org/10.2514/6.2018-4998.

[4] AAMS, "AAMS Fact Sheet and FAQs," , 2020. URL https://aams.org/member-services/fact-sheet-faqs/.

[5] Brito, C., "Dramatic Video Shows Helicopter Rescue of Injured Woman Spinning Wildly Out of Control," , June 2019. URL https://www.cbsnews.com/news/helicopter-rescue-spinning-phoenix-arizona-piestewa-peak-stretcher/.

[6] Bledsoe, B., "EMS Myth #6: Air Medical Helicopters Save Lives and are Cost-Effective," , 2003. URL https://www.emsworld.com/article/10325077/ems-myth-6-air-medical-helicopters-save-lives-and-are-cost-effective.

[7] Kupas, D. F., "Lights and Siren Use by Emergency Medical Services (EMS): Above All Do No Harm," Tech. rep., U.S. Department of Transportation: National Highway Traffic Safey Administration Office of Emergency Medical Services (EMS), 2017.

[8] FAA, "Risk Management Handbook," , 2016. URL https://www.faa.gov/regulations_policies/handbooks_manuals/aviation/media/risk_management_hb_change_1.pdf.

[9] Lilium, "Lilium: The Jet," https://lilium.com/the-jet, 2020.

[10] Airbus, "CityAirbus - Urban Air Mobility - Airbus," https://www.airbus.com/innovation/zero-emission/urban-air-mobility/cityairbus.html, 2020.

[11] Aurora Flight Sciences, "PAV eVTOL Passenger Air Vehicle," https://www.aurora.aero/pav-evtol-passenger-air-vehicle/, 2020.

[12] Electric VTOL News, "Hyundai S-A1," https://evtol.news/hyundai-s-a1/, 2020.

[13] Uber, "Uber Elevate | Uber Air," https://www.uber.com/us/en/elevate/uberair/, 2020.

[14] Kittyhawk Aero, "Kittyhawk Heaviside," https://kittyhawk.aero/heaviside/, 2020.

[15] Blain, L., "Australian eVTOL Prototype Debuts a New Spin on the Tilt Rotor," https://newatlas.com/aircraft/amsl-vertiia-australian-evtol-air-taxi-prototype/, Nov. 2020.

[16] Bacchini, A., and Cestino, E., "Electric VTOL Configurations Comparison," *Aerospace*, Vol. 6, No. 3, 2019, p. 26. https://doi.org/10.3390/aerospace6030026.

[17] Shi, X., Veismann, M., Dougherty, C. J., Rider, S., Chung, S.-J., Gharib, M., Kim, K., Rahili, S., and Nemovi, R., "Autonomous Flying Ambulance," , Pending U.S. Patent US20190106206A1, April 2019.

[18] Gordon, C. C., Blackwell, C. L., Bradtmiller, B., Parham, J. L., Barrientos, P., Paquette, S. P., Corner, B. D., Carson, J. M., Venezia, J. C., Rockwell, B. M., Mucher, M., and Kristensen, S., "2012 Anthropometric Survey of U.S. Army Personnel: Methods and Summary Statistics," Tech. Rep. NATICK/TR–15/007, U.S. Army Natick Soldier Research, Development and Engineering Center, Natick, Massachusetts, 2012.

[19] Reuters, "Air Taxi Startup Lilium's First U.S. Hub to be in Florida," https://www.reuters.com/article/us-aviation-taxis-lilium/air-taxi-startup-liliums-first-u-s-hub-to-be-in-florida-idUSKBN27R25O, Nov. 2020.

[20] Wolowicz, C. H., and Bowman, J. S., "Similitude Requirements and Scaling Relationships as Applied to Model Testing," Tech. Rep. TP 1435, NASA, 1979. URL https://ntrs.nasa.gov/citations/19790022005.

[21] Shi, X., Spieler, P., Tang, E., Lupu, E.-S., Tokumaru, P. T., and Chung, S.-J., "Adaptive Nonlinear Control of Fixed-Wing VTOL with Airflow Vector Sensing," *Proc. IEEE International Conference on Robotics and Automation (ICRA)*, 2020.

[22] Shi, G., Shi, X., O'Connell, M., Yu, R., Azizzadenesheli, K., Anandkumar, A., Yue, Y., and Chung, S.-J., "Neural lander: Stable drone landing control using learned dynamics," *Proc. IEEE International Conference on Robotics and Automation (ICRA)*, 2019, pp. 9784–9790.

[23] Rivière, B., Hönig, W., Yue, Y., and Chung, S.-J., "GLAS: Global-to-Local Safe Autonomy Synthesis for Multi-Robot Motion Planning with End-to-End Learning," *IEEE Robotics and Automation Letters*, Vol. 5, No. 3, 2020, pp. 4249–4256.

[24] Nakka, Y. K., Liu, A., Shi, G., Anandkumar, A., Yue, Y., and Chung, S.-J., "Chance-Constrained Trajectory Optimization for Safe Exploration and Learning of Nonlinear Systems," *IEEE Robotics and Automation Letters*, 2020. In press.

[25] Kim, K., Rahili, S., Shi, X., Chung, S.-J., and Gharib, M., "Controllability and Design of Unmanned Multirotor Aircraft Robust to Rotor Failure," *AIAA Scitech 2019 Forum*, AIAA, 2019. https://doi.org/10.2514/6.2019-1787.

[26] Raymer, D., *Aircraft Design: A Conceptual Approach*, American Institute of Aeronautics and Astronautics, Inc, Reston, Virginia, 2018.

[27] NASA, "OpenVSP," http://openvsp.org/, 2020.

[28] Simons, M., *Model Aircraft Aerodynamics*, 5th ed., Special Interest Model, Poole, 2014.

[29] Selig, e. a., M.S, "Summary of Low-Speed Airfoil Data (Vol. 1, 2 and 3)," https://m-selig.ae.illinois.edu/uiuc_lsat.html, 1995-1997. SoarTech Publications.

[30] Gudmundsson, S., *General Aviation Aircraft Design: Applied Methods and Procedures*, Butterworth-Heinemann, Oxford Waltham, MA, 2014.

[31] Raymer, D. P., Wilson, J., Perkins, H. D., Rizzi, A., Zhang, M., and Puentes, A. R., "Advanced Technology Subsonic Transport Study: N+3 Technologies and Design Concepts," Tech. Rep. NASA/TM 2011-217130, NASA, 2011.

[32] Sahwee, Z., Kamal, N. L. M., Hamid, S. A., Norhashim, N., Lott, N., and Asri, M. H. M., "Drag Assessment of Vertical Lift Propeller in Forward Flight for Electric Fixed-Wing VTOL Unmanned Aerial Vehicle," *IOP Conference Series: Materials Science and Engineering*, Vol. 705, 2019, p. 012007. https://doi.org/10.1088/1757-899x/705/1/012007.

[33] Stahl, P., Rössler, C., and Hornung, M., "Benefit Analysis and System Design Considerations for Drag Reduction of Inactive Hover Rotors on Electric Fixed-Wing VTOL Vehicles," *2018 Aviation Technology, Integration, and Operations Conference*, American Institute of Aeronautics and Astronautics, 2018. https://doi.org/10.2514/6.2018-4150.

[34] Aeroandi.de, "Floater4 VTOL Drone," http://aeroandi.de/planes-drones/floater4-vtol-drone/, 2020.